Femtosecond Time-Resolved Absorption Spectroscopy of Astaxanthin in Solution and in -Crustacyanin

Robielyn P. Ilagan,[†] Ronald L. Christensen,[‡] Timothy W. Chapp,[†] George N. Gibson,[§] Torbjorn Pascher,[⊥] Tomáš Polívka,[⊥] and Harry A. Frank*,[†]

Department of Chemistry, Uni ersity of Connecticut, Storrs, Connecticut 06269-3060, Department of Chemistry, Bowdoin College, Brunswick, Maine 04011-8466, Department of Physics, Uni ersity of Connecticut, Storrs, Connecticut 06269-3046, and Department of Chemical Physics, Lund Uni ersity, Box 124, S-22100 Lund, Sweden

Recei ed: December 8, 2004; In Final Form: February 8, 2005

Steady-state absorption and femtosecond time-resolved spectroscopic studies have been carried out on astaxanthin dissolved in CSf

$_2$ and $S_1 \rightarrow S_n$ transitions. Planarization of the astaxanthin molecule, which leads to a longer effective π-electron conjugated chain and a lower S_1 energy, accounts for the shorter τ_1 in the protein.

Introduction

The species of lobster indigenous to North America, *Homarus americanus*, and its European North Sea relative, *Homarus gammarus*

structure by Cianci et al.[27] has spawned several theoretical and experimental investigations to explain the bathochromic shift of the absorption spectrum of the astaxanthin molecule induced upon binding to the crustacyanin protein.

Prior to the report of the β-crustacyanin crystal structure, Weesie et al.[10] used a combination of classical molecular

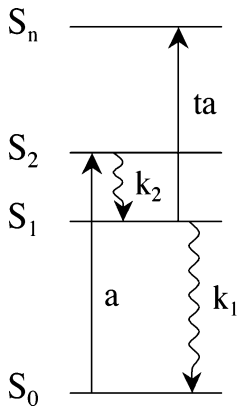

Figure 3. Energy level scheme for astaxanthin. a is absorption and ta is transient absorption. k_1 and k_2 are rate constants associated with the decay of S_1 and S_2, respectively.

mainly to hydrogen bonding of the astaxanthin keto groups to histidine residues and water molecules in the protein. The effect of the histidine was found to be directly dependent on the astaxanthin protonation state.[11] Even more recently, van Wijk et al.[12] used TDDFT calculations on several models based on the X-ray structure of β-crustacyanin to complement their results on ^{13}C NMR and resonance Raman spectroscopy on the ^{13}C-labeled astaxanthins. They postulated that the conformational twisting of astaxanthin induced by protein binding and hydrogen bonding account for only one-third of the total bathochromic shift in -crustacyanin. They suggested that the spectral properties of -crustacyanin are determined to a much larger extent by exciton interactions between proximal chromophores.[12] Moreover, the circular dichroism spectrum of β-crustacyanin has been interpreted in terms of exciton splitting between the two twisted astaxanthins.[6,22,28]

In this paper we present ultrafast time-resolved spectroscopic studies of astaxanthin in solution and in -crustacyanin. This protein complex is one of only a few well-characterized carotenoproteins that do not bind chlorophyll.[24] Thus, the data presented here are important for understanding the intrinsic behavior of carotenoids in a protein environment in the absence of interactions with chlorophyll, which typically would result in excited-state energy transfer between these cofactors. The comparison of the results from -crustacyanin with those obtained for astaxanthin in solution reveals how the binding of the molecule to the -crustacyanin protein alters its photophysical behavior. This information is essential for understanding the factors controlling the optical spectroscopy of protein-bound carotenoids.

Materials and Methods

Sample Preparation. Astaxanthin was obtained from Roche and was purified with use of a Millipore Waters 600E high-performance liquid chromatography (HPLC) system equipped with a photodiode array detector. The mobile phase consisted of an isocratic mixture of 11:89 v/v methyl *tert*-butyl ether (MTBE):methanol with a flow rate of 0.5 mL/min on a 3.9 mm $\times$ 300 mm Nova Pak C_{18} column. The purified astaxanthin was dried with a gentle stream of nitrogen gas and then redissolved in carbon disulfide (99+% anhydrous), methanol (99.9% A.C.S. spectrophotometric grade), or acetonitrile (99.5+% spectrophotometric grade). All solvents were obtained from Sigma-Aldrich and used without further purification. The -crustacyanin was obtained as a gift from Dr. George Britton and purified prior to the spectroscopic experiments by applying the sample to a diethylaminoethyl (DEAE) cellulose column equilibrated with 50 mM potassium phosphate buffer, pH 7. The sample was eluted from the column with 0.1 M KCl in the same buffer.[5]

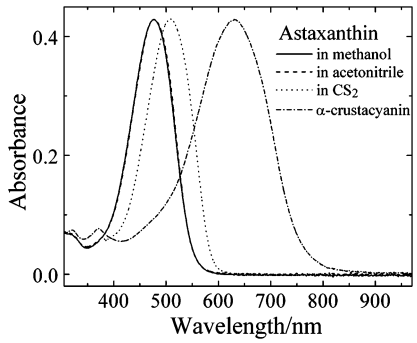

Figure 4. Normalized absorption spectra of astaxanthin in methanol, acetonitrile, CS_2, and -crustacyanin at room temperature. The spectra in methanol and acetonitrile are essentially superimposable.

Spectroscopy. The optical density of the samples was adjusted to approximately 0.4 at the excitation wavelength in a 2 mm path length cuvette. All transient absorption experiments were carried out at room temperature. The femtosecond transient absorption spectrometer system employs a Spectra-Physics Tsunami mode-locked Ti:sapphire oscillator pumped with a continuous wave, diode-pumped, Nd:YVO4 laser (Millennia, Spectra Physics). The output is amplified by a 1 kHz tunable Spitfire Ti:sapphire regenerative amplifier pumped by an Evolution Nd:YLF pump laser which generates $\sim$45 fs pulses with an average energy of 800 mJ/pulse at 800 nm. The output beam is passed through a splitter in which most of beam is used to pump the optical parametric oscillator (OPA-800) to generate the excitation wavelength. The OPA-800 produces signal and idler outputs up to 100 μJ and, for the experiments reported here, used a beta-barium borate (BBO) Type I crystal to produce excitation wavelengths from 500 to 600 nm by harmonic generation or sum frequency mixing. The rest of the output beam is used to generate white light continuum probe pulses by using a sapphire plate contained in an Ultrafast System LLC spectrometer. The excitation and probe pulses were overlapped at the sample with their relative polarization set to the magic angle (54.7°). A polarizer was placed before the charge-coupled device (CCD) detector to minimize the scattered signal from the pump pulse. Excitation was 540 nm for astaxanthin in CS_2, 500 nm for astaxanthin in methanol and acetonitrile, and 600 nm for the -crustacyanin sample. The assignment of time zero was based on the maximum temporal overlap of the pump and the probe pulses. The dynamics showed no dependence on excitation energy from 0.2 to 2.0 μJ/pulse. The sample was stirred with a magnetic microstirrer to avoid sample photodegradation. Absorption spectra of the samples were taken at room temperature to confirm sample integrity before and after the transient absorption experiments. A MatLab program was used to correct for the dispersion in the transient absorption spectra.

Results

Astaxanthin in methanol, acetonitrile, CS_2, and -crustacyanin displays broad, featureless steady-state absorption spectral line shapes (Figure 4). In methanol and acetonitrile, astaxanthin absorbs at 476 nm, whereas in CS_2 the maximum absorption is at 506 nm. This red-shift can be attributed to the higher polarizability of CS_2, which lowers the $S_0 \rightarrow S_2$ transition energy more than the other solvents. Astaxanthin in -crustacyanin has an absorption maximum at approximately 630 nm, which accounts for the characteristic blue color of this pigment.

The transient absorption spectra taken 1.0 ps after excitation for astaxanthin in methanol, acetonitrile, CS_2, and -crustacyanin are shown in Figure 5. As for the ground-state absorption (Figure 4), a large spectral shift is observed for astaxanthin in -crustacyanin compared to the molecule in solution. Parts A and C of Figure 6 show the instantaneous bleaching and subsequent recovery of the ground-state absorption that occurs after the excitation pulse for astaxanthin in CS_2 and -crustacyanin. The recovery of the ground-state absorption in -crustacyanin (Figure 6C) is faster than that for astaxanthin in CS_2 (Figure 6A). The rise and decay of the $S_1 \rightarrow S_n$ transient absorption (Figure 6B,D) is observed to the red of the signal associated with the bleaching of the ground state. The decay of the transient absorption signal observed for the -crustacyanin protein also is faster than that observed for astaxanthin in solution (compare part D with part B in Figure 6).

Transient spectra for astaxanthin in CS_2 and -crustacyanin taken at various time delays are shown in Figures 7A and 8A. The spectra shown in Figure 7A are typical of the results from all the solvents. The transient spectra show a broad bleaching in the 450 575 nm region that corresponds to the disappearance of the $S_0 \rightarrow S_2$ absorption band upon excitation. Subsequently, there is a buildup of an excited-state absorption signal in the 575 800 nm region corresponding to an $S_1 \rightarrow S_n$ transition. Virtually identical features are observed for astaxanthin in -crustacyanin except for the fact that both the bleaching and excited state absorption signals from this sample (Figure 8A) are red-shifted by approximately 100 nm compared to those seen for astaxanthin in CS_2 (Figure 7A).

The transient dynamics from all the samples were analyzed by using the kinetic model given in Figure 3. The rate equations are

where $[S_i]$ is the normalized population of the S_i level, t is time, σ_N is the absorption cross section, τ_s is the instrument response time, I_0 is the peak pump intensity (in photons/cm^2 s), and k_1 and k_2 are decay rate constants for the transitions $S_1 \rightarrow S_0$ and $S_2 \rightarrow S_1$, respectively. The solution to the set of coupled differential equations assumed that the total population in the states, S_0, S_1, and S_2, remained constant over all time and that at negative infinite time, all the population was in the ground state, S_0. The excitation of the molecules via the $S_0 \rightarrow S_2$ transition was assumed to be instantaneous. The percent population decaying directly via $S_2 \rightarrow S_0$ relaxation was assumed to be negligible compared to decay of S_2 via $S_2 \rightarrow S_1$. Integrating eq 1 gives the time dependence of the ground state, S_0, population, which can be used to fit the kinetics of the bleaching of the $S_0 \rightarrow S_2$ transition (Figure 6A,C). The time dependence of the S_1 state population is derived from the coupled set of eqs 1dep (1)Tj 9.479 0 0 9.479 90.355 368.759 Tm [(,)-534(a3294 -1479 133.518 346.808 Tm oupled808 Tm oupled80hhe)-335(chhe)-335(chhe

improved by adding a third decay component. The time constants obtained for these experiments were $\tau_1 = 4.3 \pm 0.3$ ps, $\tau_2 = 145 \pm 50$ fs, and $\tau_3 = 1.9 \pm 0.4$ ps. The amplitude spectra constructed from the wavelength dependence of the preexponential factors, $A_i(\lambda)$ (eq 7), of these components are shown in Figure 7B. The negative values of the 145 fs component in the spectral region of the $S_1 \rightarrow S_n$ band (550 to 750 nm) indicate that this component is due to a rise of the $S_1 \rightarrow S_n$ band and thus can associated with $S_2 \rightarrow S_1$ relaxation. The 4.3 ps component is associated with the decay of the $S_1 \rightarrow S_n$ band and the recovery of the ground-state bleaching (Figure 4) and corresponds to the S_1 lifetime. On the other hand, the spectral profile of the 1.9 ps component suggests that it has its origin in a blue-shift of the $S_1 \rightarrow S_n$ band because it decays on the red side of the $S_1 \rightarrow S_n$ band, while a negative value on the blue side of this band indicates a 1.9 ps rise in this spectral region. In addition, the larger negative amplitude of this component at 560 nm suggests that it is connected with a formation of the shoulder located at 560 nm, which is clearly visible in the transient absorption spectra at later delay times (e.g. spectrum f in Figure 7A). Such behavior is consistent with equilibration in the S_1 state, but the origin of this process is not easy to discern. It does not seem to be due to S_1 vibrational relaxation, for which a large blue shift and narrowing is observed.[30,31] The behavior of the 1.9 ps component is reminiscent of that observed for peridinin, which was ascribed to equilibration between the S_1 and ICT states.[32] However, since no stabilization of the ICT state is observed for astaxanthin (see below), such an assignment can be ruled out. Other processes, such as involvement of a so-called S* state, usually exhibited as a blue shoulder at the $S_1 \rightarrow S_n$ band,[33] or excited-state solvation, which has a characteristic time constant of $\sim$2 ps for CS_2,[34] cannot be ruled out. We thus cannot unequivocally assign the 1.9 ps component to a particular process. However, it makes only a minor contribution to the excited-state dynamics, representing less than 10% of the total amplitude at any wavelength.

Similar to astaxanthin in CS_2, the dynamics of astaxanthin in -crustacyanin analyzed by global fitting required three decay components. The fastest component has a time constant of 100 fs, comparable to the time resolution of the instrument, and can be associated with the time constant for the decay of S_2 to S_1. The other two components decay in 1.8 and 0.6 ps, and their spectral profiles are shown in Figure 8B. The profile of the 1.8 ps component is consistent with $S_1 \rightarrow S_n$ absorption and confirms that the S_1 lifetime of astaxanthin in -crustacyanin is shorter than that in solution (Table 1). The 0.6 ps component

(38) Zigmantas, D.; Hiller, R. G.; Sharples, F. P.; Frank, H. A.; Sundstrom, V.; Polivka, T. *Phys. Chem. Chem. Phys.* **2004**, *6*, 3009.
(39) Polivka, T.; Kerfeld, C. A.; Pascher, T.; Sundstrom, V. *Biochemistry* **2005**, *44*, 3994.